Intermediate valence metals

Jon Lawrence, UCI Colloquium, 12 October 2006

www.physics.uci.edu/~jmlawren

1. Introduction to concept of intermediate valence (IV)
2. Anderson impurity model
   - Fits of $\chi(T)$, $n_f(T)$, $Cp(T)$, $\chi''(\omega)$ to AIM (dominated by local spin fluctuations)
   - PES(w) showing large vs. small energy scales
3. Coherent Fermi liquid ground state:
   - Transport, specific heat and Pauli susceptibility
   - De Haas van Alphen and LDA band theory
   - Optical conductivity, neutron scattering and the Anderson Lattice
4. Anomalies
   - Slow crossover from Fermi liquid to local moment
   - Low temperature susceptibility and specific heat anomalies
   - Low temperature anomaly in the spin dynamics

Collaborators:

LANL CMP: Zach Fisk, Joe Thompson, John Sarrao, Mike Hundley, Al Arko, George Kwei, Eric Bauer

NHMFL/LANL: Alex Lacerda, Neil Harrison

Argonne National Lab: Ray Osborn, Eugene Goremychkin

Brookhaven National Lab: Steve Shapiro

Shizuoka University: Takao Ebihara

UCI Postdocs: Andy Cornelius (UNLV), Corwin Booth (LBL), Andy Christianson (ORNL)

UCI students: Jerry Tang, Victor Fanelli

Temple U.: Peter Riseborough

Intermediate Valence Compounds

$CeBe_{13}$	Fermi liquid (FL)	$YbAgCu_4$
$CePd_3$	FL with anomalies	$YbAl_3$
$Ce_3Bi_4Pt_3$	Kondo Insulator	YbB_{12}
γ-α Ce	Valence transition	$YbInCu_4$

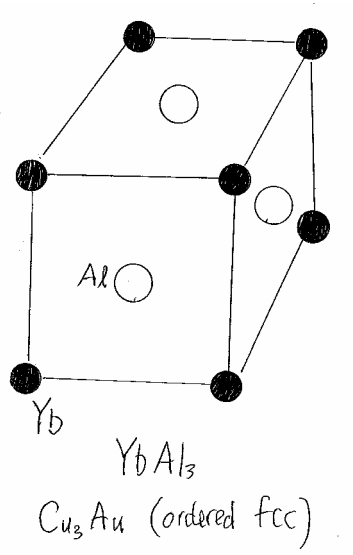

Intermediate Valence (IV) = Nonintegral valence

Yb:	$(5d6s)^3\ 4f^{13}$	$n_f = 1$ trivalent
	$(5d6s)^2\ 4f^{14}$	$n_f = 0$ divalent
$YbAl_3$	$(5d6s)^{2.75}\ 4f^{13.25}$	$n_f = 0.75$ IV
Ce:	$(5d6s)^3 4f^1$	$n_f = 1$ trivalent
	$(5d6s)^4 4f^0$	$n_f = 0$ tetravalent
$CePd_3$	$(5d6s)^{3.2} 4f^{0.8}$	$n_f = 0.8$ IV

Oversimplified single ion model:

Two nearly-degenerate localized configurations form hybridized w.f.:

$a\ [4f^{13}(5d6s)^3> + b\ [4f^{14}(5d6s)^2>$ where $a = \sqrt{n_f}$ and $b = \sqrt{(1 - n_f)}$

Basic underlying physics:

Highly localized $4f^{13}$ orbital surrounded by a sea of conduction electrons

Nearly degenerate with $4f^{14}$ orbital

Energy separation: E_f

Strong on-site Coulomb interaction U between 4f electrons; $4f^{12}$ orbital at energy $E_f + U$ where $U >> V, E_f$

Hybridization V between configurations: conduction electrons hop on and off the 4f impurity orbital. Hybridization strength

$\Gamma = V^2\rho$ where ρ is the density of final (conduction) states.

Correlated hopping:

when $\Gamma \sim E_f << U$ then

hopping from $4f^{14}$ to $4f^{13}$ is allowed

but hopping from $4f^{13}$ to $4f^{12}$ is inhibited by the large value of U.

Classic correlated electron problem!

These IV properties are captured by Anderson Impurity Model (AIM)

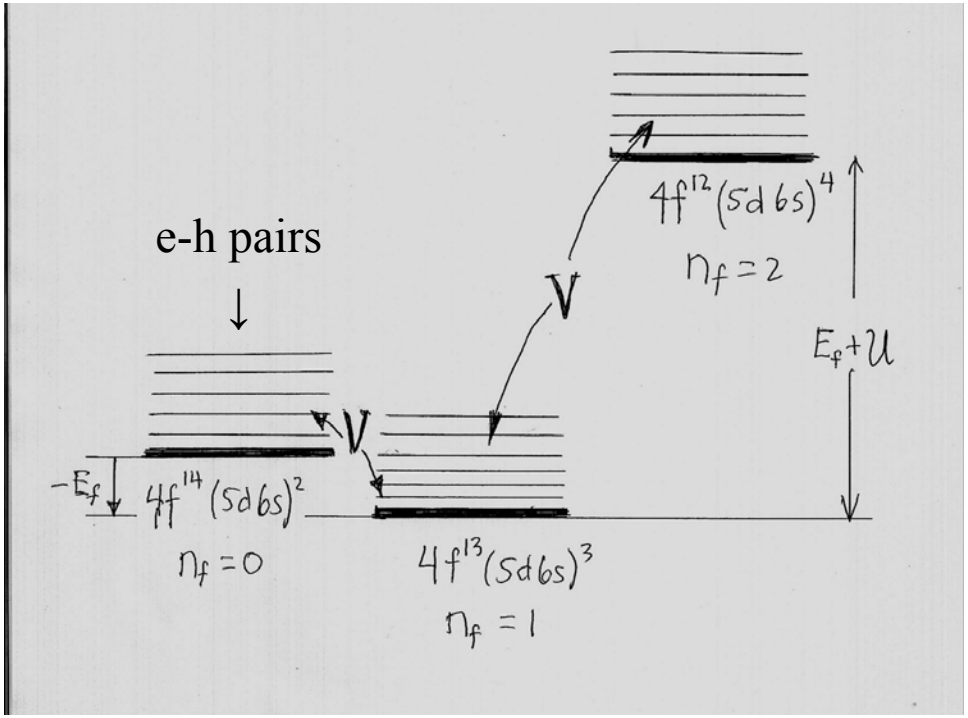

Although intended for dilute alloys,

(e.g. $Lu_{1-x}Yb_xAl_3$), because the spin fluctuations are local, the AIM describes much of the physics of periodic IV compounds.

Key predictions of Anderson Impurity model:

All approximately valid for periodic IV metals.

***Energy lowering* due to hybridization:**

$k_B T_K \sim \varepsilon_F \exp\{-E_f/[N_J V^2 \rho(\varepsilon_F)]\} \sim (1 - n_f) N_J V^2 \rho(\varepsilon_F)$

Kondo Resonance: Narrow 4f resonance at the Fermi level ε_F.

(Virtual charge fluctuations yield low energy spin fluctuations.)

Contributes to the density-of-states (DOS) as $\rho_f(\varepsilon F) \sim 1/T_K$.

***Mixed valence* due to hybridization ($n_f < 1$)**

Spin/valence fluctuation: localized, damped oscillator with characteristic energy

$E_0 = k_B T_K$: $\chi'' \sim \chi(T) E \Gamma/((E-E_0)^2 + \Gamma^2)$

Universality: Properties scale as T/T_K, $E/k_B T_K$, $\mu_B H/k_B T_K$

High temperature limit: LOCAL MOMENT PARAMAGNET

Integral valence: $n_f \rightarrow 1$ $z = 2+n_f = 3$ Yb $4f^{13}(5d6s)^3$

Curie Law: $\chi \rightarrow C_J/T$ where $C_J = N g^2 \mu_B^2 J(J+1)/ 3 k_B$ $J = 7/2$ (Yb)

Full moment entropy: $S \rightarrow R \ln(2J+1)$

CROSSOVER at Characteristic temperature T_K

Low temperature limit: FERMI LIQUID

Nonintegral valence ($n_f < 1$) Yb $4f^{14-nf}(5d6s)^{2+nf}$

Pauli paramagnet: $\chi(0) \sim \mu_B^2 \rho_f(\varepsilon_F)$

Linear specific heat: $C_v \sim \gamma T$ $\gamma = (1/3) \pi^2 \rho_f(\varepsilon_F) k_B^2$

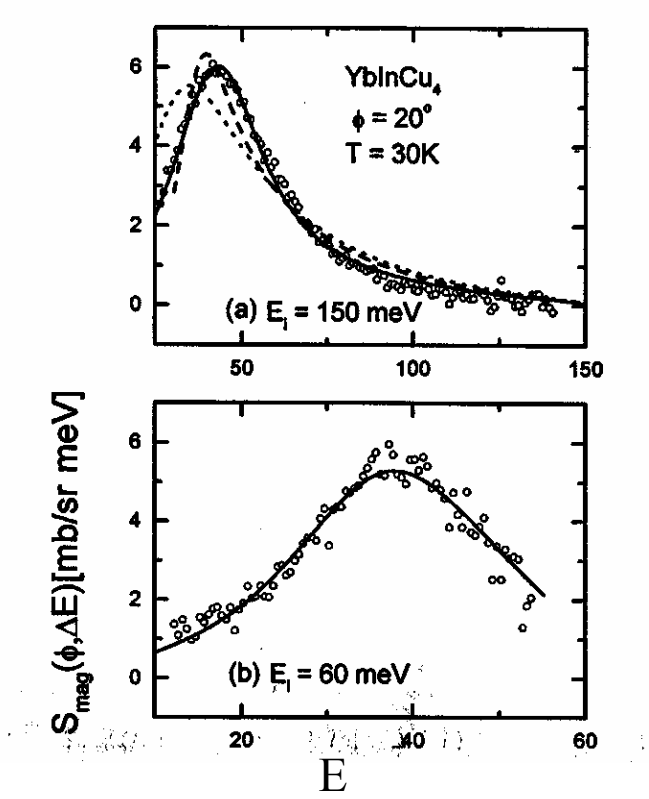

Spin fluctuation spectra $YbInCu_4$

$YbInCu_4$
Magnetic scattering
S_{mag} vs. E at two incident energies E_i

Lawrence, Osborn et al
PRB 59 (1999) 1134

Lorentzian power spectrum

$$S(E) \sim \chi' E P(E) = \chi' E (\Gamma/2)/\{(E - E_0)^2 + \Gamma^2\}$$

Q-dependence: In $YbInCu_4$ (Lawrence, Shapiro et al, PRB 55 (1997) 14467) ***no dependence of Γ or E_0 on Q*** and only a weak (15%) dependence of χ' on **Q**.

Q-independent, broad Lorentzian response $\Rightarrow$

Primary excitation is a local, highly damped spin fluctuation (oscillation) at characteristic energy $E_0 = k_B T_K$

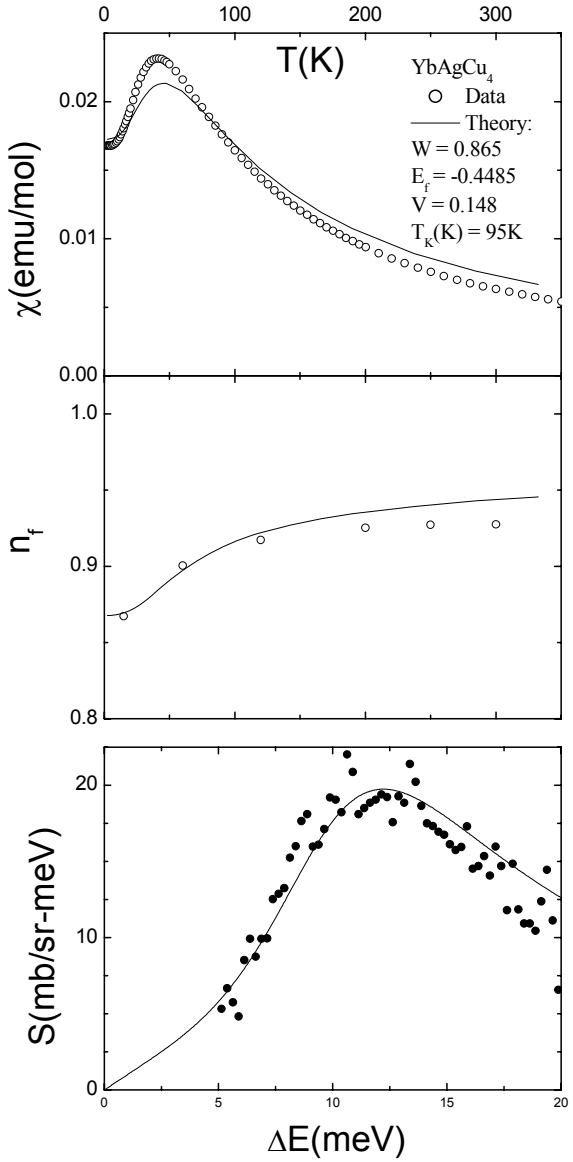

Lawrence, Cornelius, Booth, et al

Fits to the AIM

$YbAgCu_4$: *Good quantitative fits*

to the T dependence of χ, n_f, γ and to the low T neutron spectrum

O data

___ AIM

Two parameters (E_f, V) chosen to fit $\chi(0)$ and $n_f(0)$

(plus one parameter for background bandwidth W, chosen to agree with specific heat of nonmagnetic analogue $LuAgCu_4$)

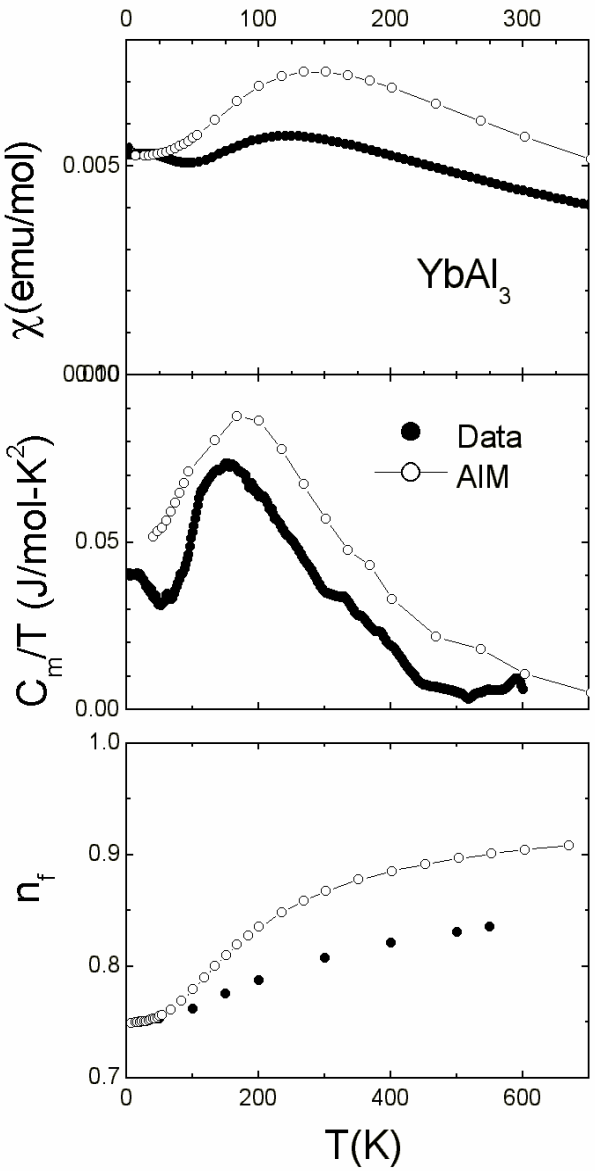

Cornelius et al
PRL 88 (2002) 117201

Comparison to AIM $YbAl_3$: Semiquantitative agreement

AIM parameters

(Chosen to fit $\chi(0)$, $n_f(0)$ and $\gamma(LuAl_3)$)

W = 4.33eV
E_f = -0.58264eV
V = 0.3425eV
T_K = 670K

The AIM predictions evolve more slowly with temperature than the data (***slow crossover*** between the Fermi liquid and the local moment regime) and there are ***low temperature anomalies*** in the susceptibility, specific heat and the neutron spectrum.

Comparison to AIM (continued)
$YbAl_3$ Spin dynamics: Neutron scattering (Q- averaged)

At T = 100K the neutron scattering exhibits an inelastic (IE) Kondo peak:

$\chi''(E) = \Gamma E / ((E- E_1)^2 + \Gamma^2)$

representing the strongly damped local excitation. For $YbAl_3$, E_1/k_B = 550 K which is of order T_K.

This Lorentzian is still present at 6 K where experiment gives

E_1 = 50 meV and Γ = 18 meV

while the AIM calculation gives

E_1 = 40meV and Γ = 22meV

(***Semiquantitative agreement***)

In addition, there is a new peak (***low temperature anomaly***) at 32 meV.

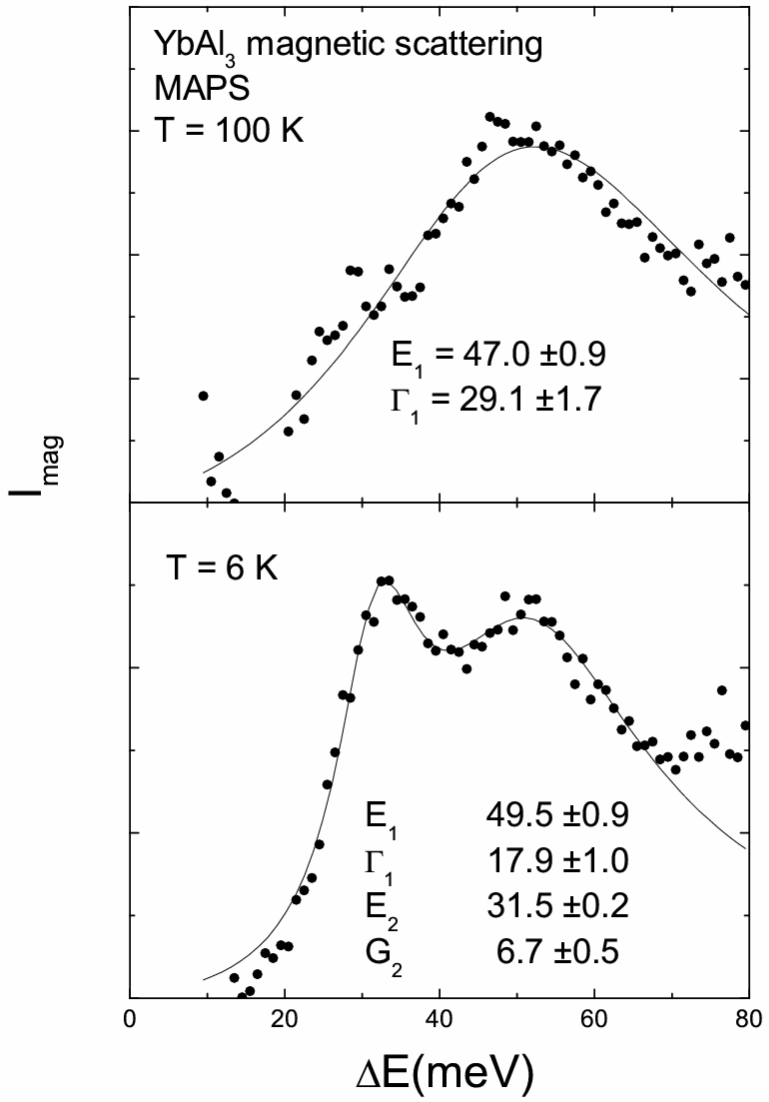

Lawrence, Christianson et al, unpublished data

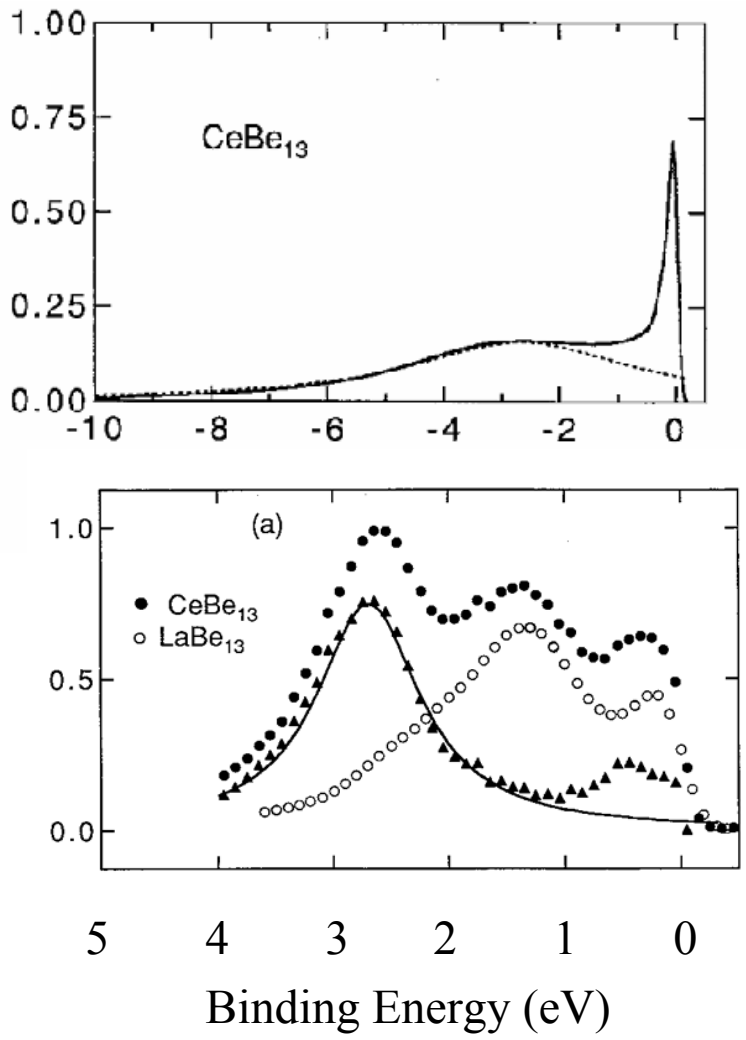

Lawrence, Arko et al PRB 47 (1993) 15460

The AIM prediction for photoemission

(Gives the relationship between large and small energy scales)

Primary $4f^1 \rightarrow 4f^0$ emission at

$-E_f \sim$ (-2.7 eV in $CeBe_{13}$)

Hybridization width 1 eV = $N_J V^2 \rho(\varepsilon_F)$

{implies $\exp[-E_f/ (N_J V^2 \rho(\varepsilon_F))] = 0.066$}

Kondo Resonance near Fermi energy ε_F

w/ width proportional to T_K.

Qualitative agreement, but there is a long-standing argument about the details:

E.g. the relative weight in the KR is larger than expected, suggesting the 4f electrons are forming narrow bands near ε_F.

The temperature dependence is also not as predicted, (perhaps "slow crossover")

Many problems arise from the high surface sensitivity of the measurement.

TRANSPORT BEHAVIOR OF IV COMPOUNDS

The AIM predicts a finite resistivity at T = 0 due to unitary scattering from the 4f impurity.

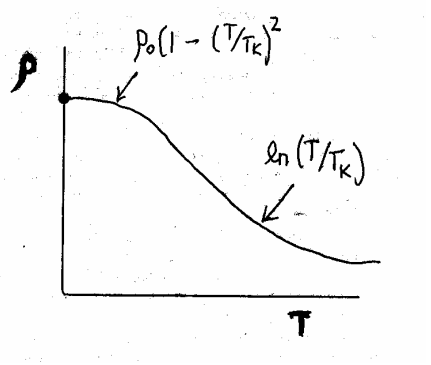

In an IV compound, where the 4f atoms form a periodic array, the resistivity must vanish.

(**Bloch's law**)

Typically in IV compounds

$\rho \sim A\,(T/T_0)^2$

This is a sign of ***Fermi Liquid "coherence"*** among the spin fluctuations.

$YbAl_3$ ρ vs T^2

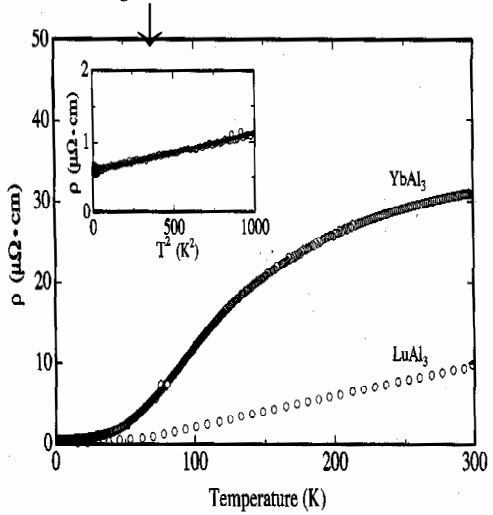

Fig. 1. Temperature dependence of the electrical resistivity of $YbAl_3$ and $LuAl_3$. The inset shows the T^2-dependence of the resistivity.

Ebihara et al
Physica B 281&282 (2000) 754

FERMI LIQUID BEHAVIOR

A Fermi liquid is a metal where, despite the strong electron-electron interactions, the statistics at low T are those of a free (noninteracting) Fermi gas, but with the replacement m $\rightarrow$ m* (the *effective mass*).

The **specific heat** is linear in temperature $C = \gamma T$

$$\gamma = \{\pi^2 k_B^2 N_A Z/(3 h^3 \pi^2 N/V)^{2/3})\} m^*$$

For simple metals (e.g. K): $\gamma = 2$ mJ/mol-K^2

$m^* = 1.25\ m_e$

For $YbAl_3$: $\gamma = 45$ mJ/mol-K^2

$m^* \sim 25\ m_e$

$\rightarrow$ "Moderately HEAVY FERMION" compound

The Fermi liquid also exhibits **Pauli paramagnetism:**

$YbAl_3$: $\chi(0) = 0.005$ emu/mol

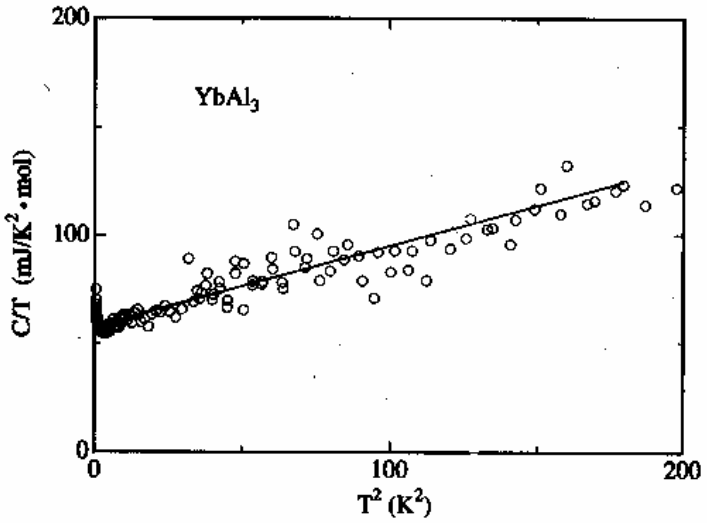

C/T vs. T^2 for $YbAl_3$

$\gamma = 45$ mJ/mol-K^2

Ebihara et al
Physica B 281&282
(2000) 754

The AIM is qualitatively good (and sometimes quantitatively, e.g. $YbAgCu_4$)
for χ (T), $C_v(T)$, $n_f(T)$ and $\chi''(\omega;T)$
essentially because these quantities are dominated by spin fluctuations, which are highly local.

BUT: to get the correct transport behavior and the coherent Fermi Liquid behavior

$\Rightarrow$ Theory must treat the 4f lattice

Two theoretical approaches to the Fermi Liquid State

Band theory: Itinerant 4f electrons: Calculate band structure in the LDA.

One-electron band theory (LDA) treats 4f electrons as itinerant;

it does a good job of treating the 4f-conduction electron hybridization.

It correctly predicts the topology of the Fermi surface.

But: ***Band theory strongly underestimates the effective masses!***

LDA: $m^* \sim m_e$ dHvA: $m^* \sim$ 15-25 m_e

And, it can't calculate the temperature dependence.

Anderson Lattice Model: Localized 4f electrons

Put 4f electrons, with AIM interactions (E_f, V, U), on each site of a periodic lattice.

This loses the details of the Fermi surface

but gets the effective masses and the T-dependence correctly.

Bloch's law is satisfied for both cases.

De Haas van Alphen and the Fermi surface

Figures from Ebihara et al, J Phys Soc Japan 69 (2000) 895

The **de Haas van Alphen** experiment measures oscillations in the magnetization as a function of inverse magnetic field.

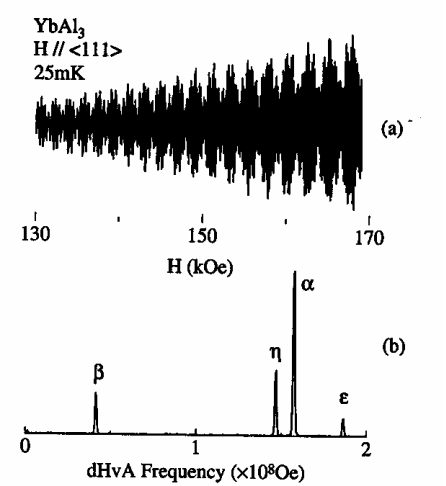

ig. 1. (a) DHvA oscillation and (b) its FFT spectrum for the field along ⟨111⟩ in $YbAl_3$.

The frequency of the oscillations is determined by the areas S of the extremal cross sections of the Fermi surface in the direction perpendicular to the applied field.

$$M = A \cos(2\pi F/H)$$

$$F = (hc/2\,\pi e)\, S$$

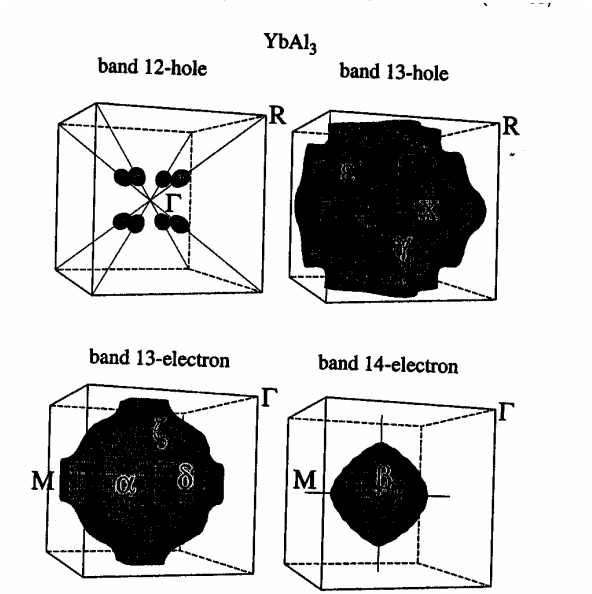

Fig. 7. Modified Fermi surfaces in $YbAl_3$. The band 13-hole and the band 13-electron Fermi surface represent the same Fermi surface.

The temperature dependence of the amplitude determines the effective mass m*

$$A = 1/\sinh(Qm^*T/H)$$

where Q is a constant

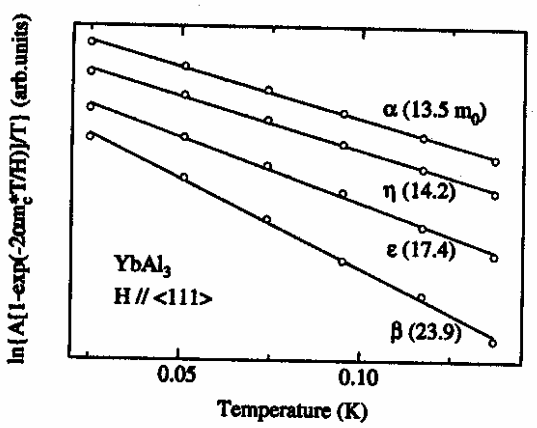

Fig. 3. Mass plot for the field along ⟨111⟩ in $YbAl_3$.

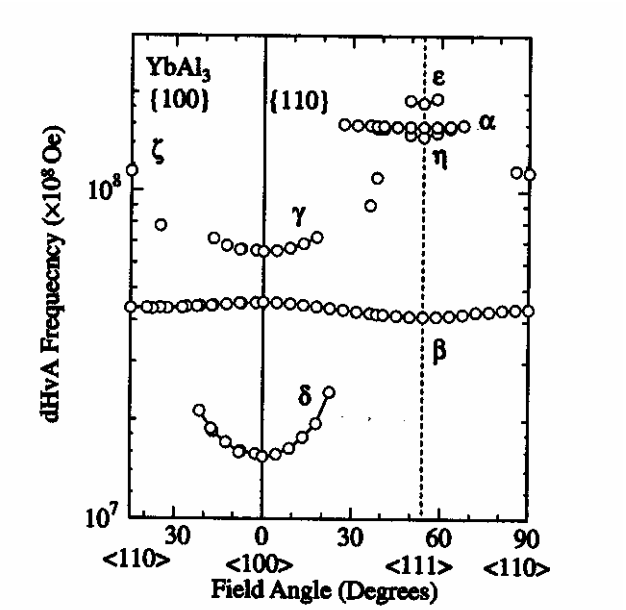

Fig. 2. Angular dependence of the dHvA frequency in $YbAl_3$.

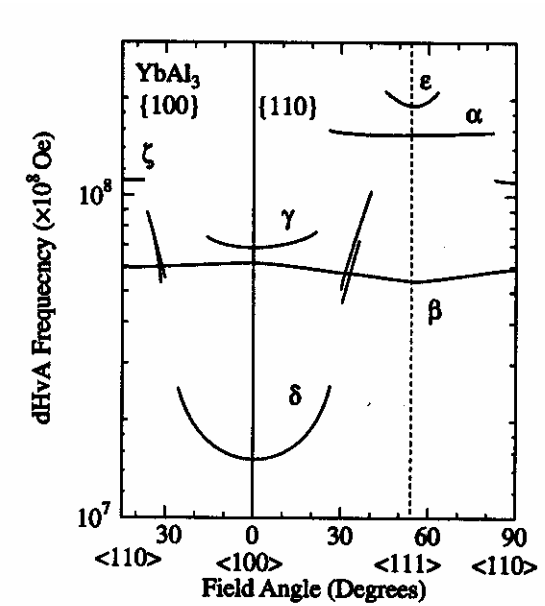

For IV compounds LDA gives the correct extremal areas!

One-electron band theory (LDA) treats 4f electrons as itinerant.
It correctly predicts the topology of the Fermi surface as observed by dHvA.

But: **LDA strongly underestimates the effective masses!**

LDA badly overestimates the 4f band widths and consequently strongly underestimates the effective masses:

LDA: $m^* \sim m_e$

dHvA: $m^* \sim 15\text{-}25 m_e$

Large effective masses in $YbAl_3$

Ebihara, Cornelius, Lawrence, Uji and Harrison

cond-mat/0209303

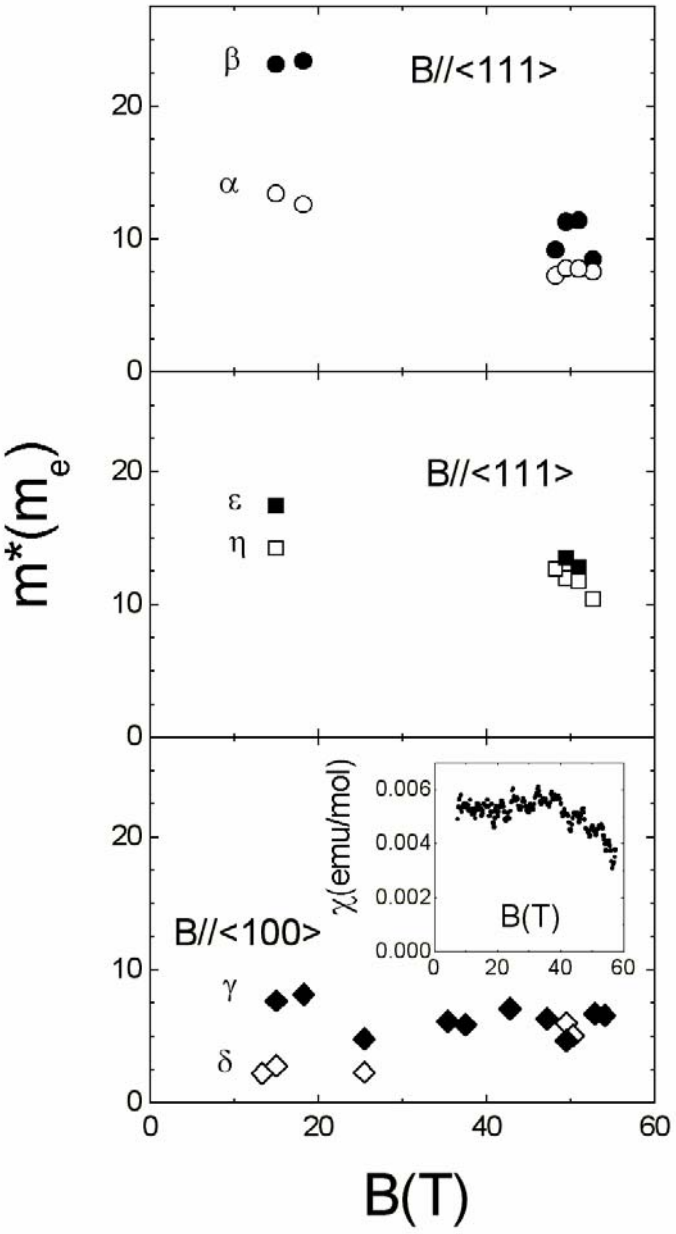

The effective masses:
Band 14 electron branch β: 23 me
Band 13 hole branch ε: 17 me
Band 13 electron branch α: 13 me

High field dHvA shows that the effective masses for H//<111> decrease substantially for H > 40T. This field is much smaller than the Kondo field $B_K = kT_K/gJ\mu_B$ required to polarize the f electrons, but is of order k_BT_{coh}/μ_B.

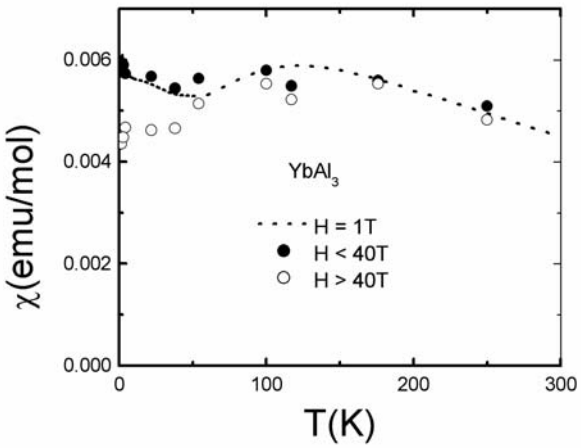

A field of this magnitude also suppresses the low temperature susceptibility anomaly.

ANDERSON LATTICE

Anderson Impurities on a periodic lattice

Level crossing: Narrow 4f band at energy E_f below the Fermi level ε_F
hybridizing, with matrix element V, with
wide conduction band whose density of states is ρ.

With no Coulomb correlations (U = 0): hybridization/level repulsion
Band structure with a hybridization gap $\Delta = N_J V^2 \rho$.

With Coulomb correlations ($U \neq 0$): U inhibits free hopping
Coherent band structure has hybridized bands near ε_F
but ***renormalized parameters***: $V_{eff} = (1-n_f)^{1/2}$ V and $U_{eff} = 0$.
Hybridization gap Δ_{eff} with indirect gap of order $T_K << \Delta$
Fermi level in high DOS region giving large m*.

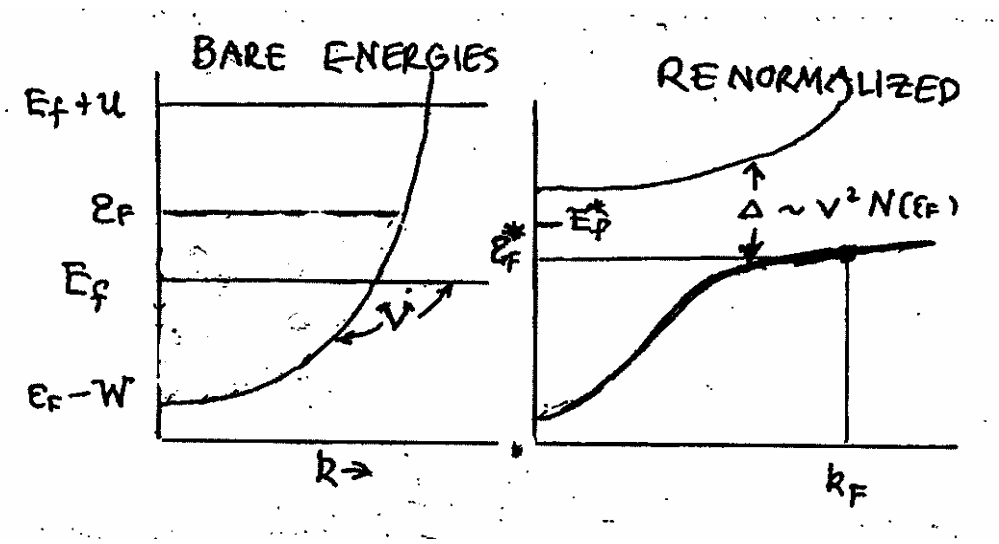

The structure renormalizes back to the bare energies with increasing temperature:

For very low $T << T_K$, fully hybridized bands.

For $T >> T_K$, local moments uncoupled from band electrons.

Optical conductivity

BEST EVIDENCE FOR THE HYBRIDIZATION GAP AND ITS RENORMALIZATION WITH TEMPERATURE

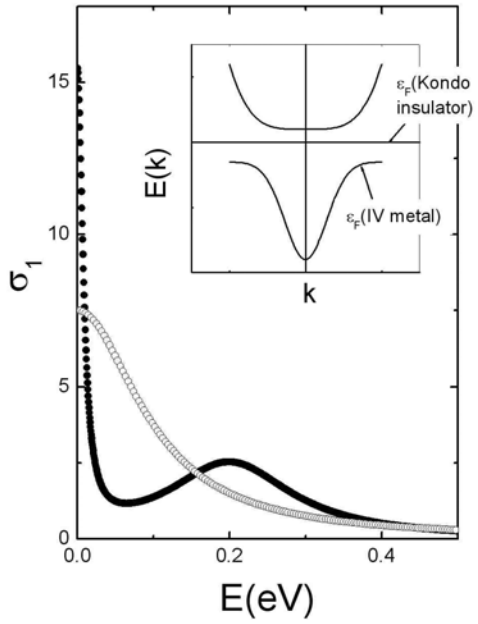

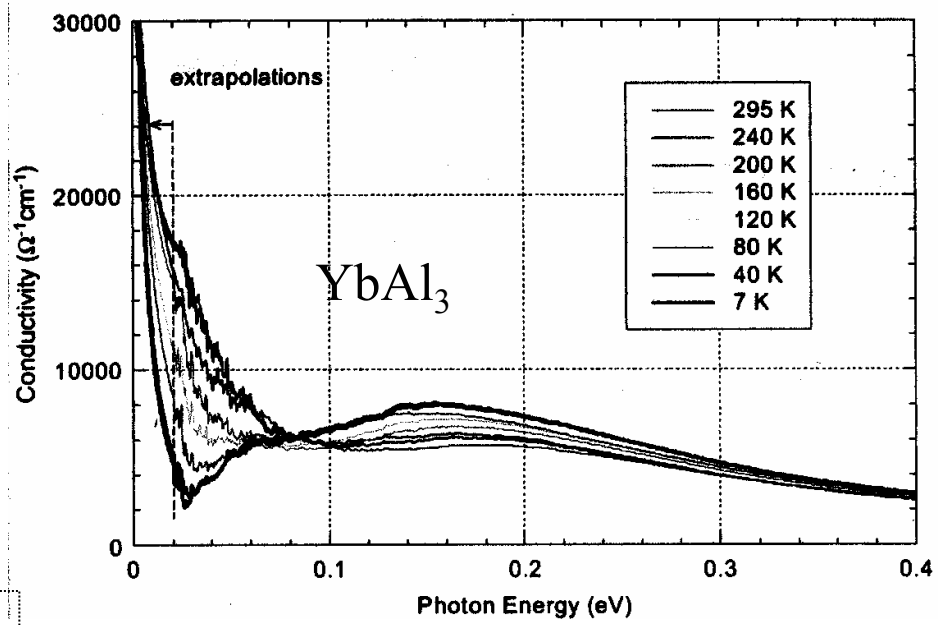

Okamura et al, J Phys Soc Japan 73 (2004) 2045

High temperature:

Normal Drude behavior from scattering from local moments:

$\sigma'(\omega) = (ne^2/m_b)\{\tau / (1 + \tau^2\omega^2)\}$

m_b: bare band mass, τ is the relaxation

CROSSOVER

Low temperature:

IR absorption peak from vertical (Q = 0) transitions across hybridization gap

Very narrow Drude peak. Both m and τ renormalized: $m_b \rightarrow \lambda\, m_b = m^*$

$\tau \rightarrow \lambda\, \tau = \tau^*$

Neutron Scattering

Both interband (across the gap) and intraband (Drude-like scattering near the Fermi energy) are expected in the neutron scattering, but in this case excitations at energy transfer ΔE can have finite momentum, transfer $\boldsymbol{Q}$.

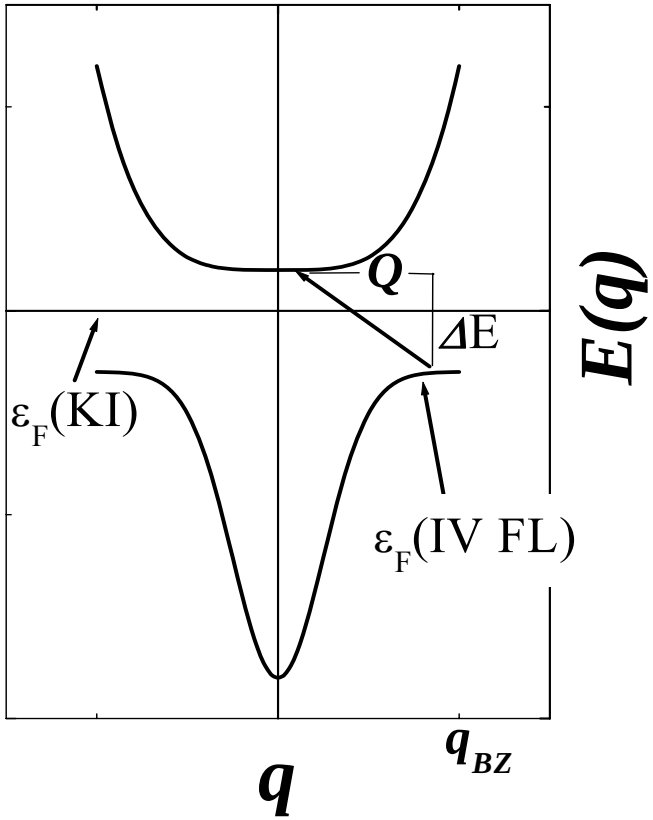

The intergap excitations, whose intensities are proportional to the joint (initial and final) density of states (DOS), should be biggest for zone boundary $\boldsymbol{Q}$ which connects regions of large 4f DOS. The energy for this case is the indirect gap. For smaller Q, the spectrum should be more like the optical conductivity (Q = 0), i.e. on the scale of the direct gap.

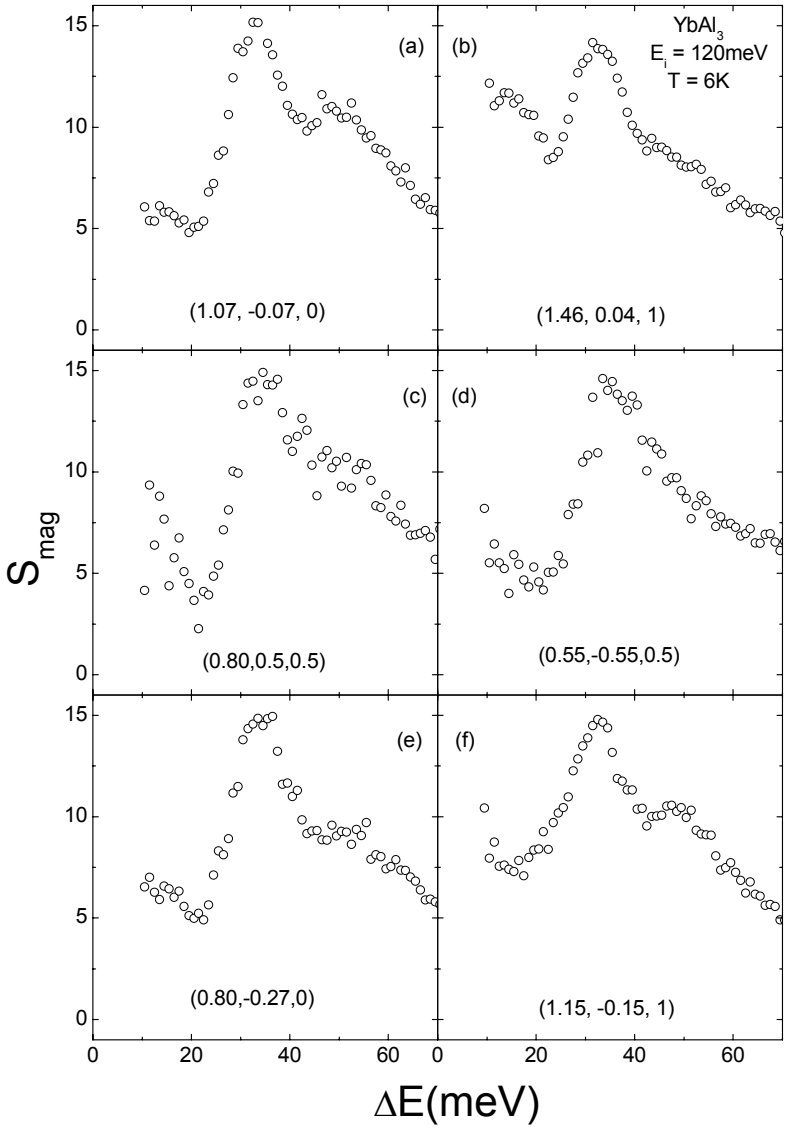

Christianson et al, PRL 96 (2006) 117206

Neutron scattering $YbAl_3$ (Q-resolved)

The low temperature magnetic scattering shows two features:

1) A broad feature near $E_1 = 50$ meV, which energy is essentially $k_B T_K$. This is most intense for zone boundary ***Q***.

2) A narrow feature near $E_2 = 30$ meV, the energy of the deep minimum in the optical conductivity. This is independent of Q.

Neutron scattering $YbAl_3$: Q dependence

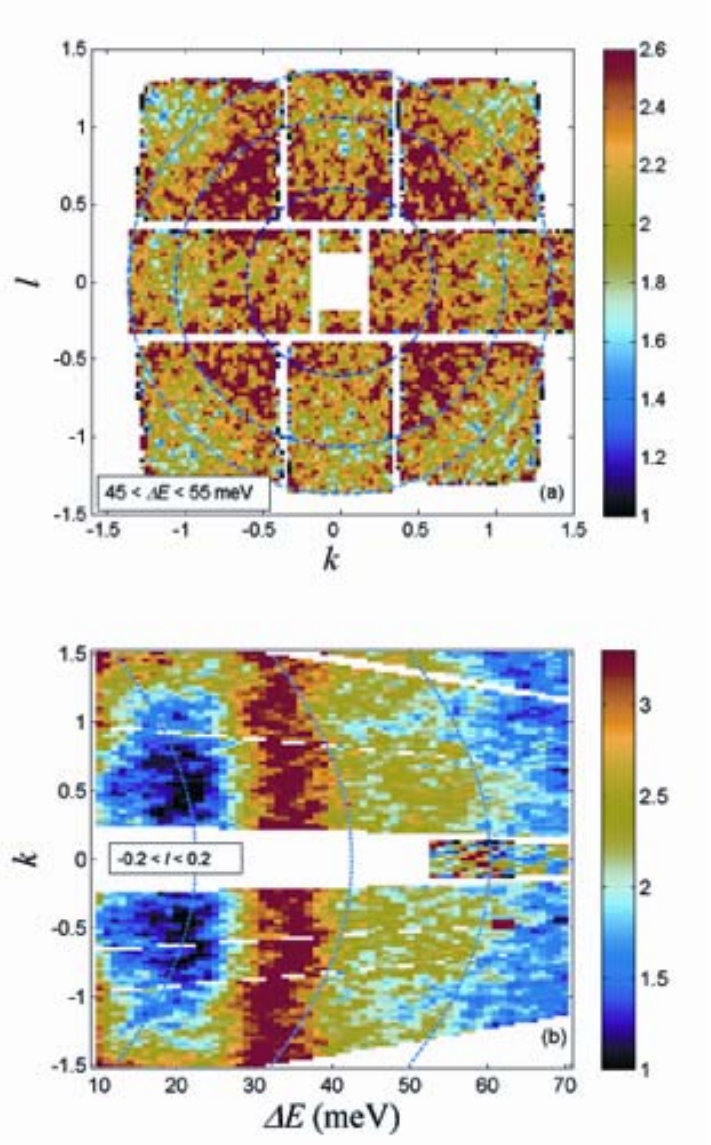

Christianson et al, PRL 96 (2006) 117206

This plot integrates over the $E_1 = 50$ meV intergap excitation at various positions in the Q_K, Q_L scattering plane. Peak intensity occurs near

$$(Q_K,Q_L) = (1/2, 1/2)$$

i.e. at the zone boundary,

This Q-dependence is as expected for intergap transitions in the Anderson lattice

This plot integrates over Q at $Q_L = 0$. The band of constant color near $E_2 = 32$ meV means that the excitation is independent of Q along the Q_K direction.

Such an excitation does not occur in the theory of the Anderson lattice. It corresponds to a localized excitation in the middle of the hybridization gap – like a magnetic exciton.

Conclusions

Properties of IV compounds such as the susceptibility, specific heat, temperature-dependent valence and Q-integrated neutron scattering line shape, which are dominated by highly localized spin fluctuations, fit qualitatively and sometimes quantitatively to the Anderson impurity model.

Properties that are highly sensitive to lattice order – d.c. transport (resistivity), optical conductivity, de Haas van Alphen – require treatment of the lattice periodicity. Band theory gets the shape of the Fermi surface correctly, but can't get the large mass enhancements or the temperature dependence. Anderson lattice theory gets the mass enhancements and the temperature dependence but forsakes the Fermi surface geometry. It predicts key features of the optical conductivity and the neutron scattering, in particular that there will be a hybridization gap, with intergap transitions strong for momentum transfer $\boldsymbol{Q}$ at the zone boundary.

However, there are many anomalies: the susceptibility and specific heat are enhanced at low T relative the models, and evolve more slowly with temperature than expected based on the AIM. In addition, there appears to be a localized excitation in the hybridization gap that is also not predicted by the models.